Thermodynamics of soil organic matter decomposition in semi-natural oak (*Quercus*) woodland in southwest Ireland.

Abstract

The thermodynamics of soil organic matter decomposition is unexplored as a way to monitor how soil organic matter changes with depth and hence with time. With that goal in mind, thermal analysis and isothermal calorespirometric measurements were made on soil samples collected at three depths in semi-natural oak woodlands at three different sites in southwest Ireland. These methods yield the enthalpy change, Gibbs energy change, and entropy change for the microbial catabolism and combustion reactions of the soil organic matter. The degree of reduction of carbon in the catabolic substrate and in the total soil organic matter was calculated from the enthalpy changes. Results show the soil organic matter becomes more reduced as decomposition proceeds from the soil organic surface to mineral soils. The top layer is characterized by high carbon content, organic materials with a low energy content per Cmole, and fast biodegradation rates. Mineral soils are characterized by low carbon content, organic materials with a high energy content per Cmole, and slow biodegradation rates. Values obtained for the entropy change were sensitive to these differences among the different soil layers. These data contribute to unlock the thermodynamics of the soil reactions and to develop the bioenergetics of soil microbial consortia in soil ecosystems.

Keywords: Thermal Analysis, calorespirometry, thermodynamics, soil, organic matter, oak.

List of symbols

C: Carbon

$\delta^{13}C$: Isotopic Carbon

ΔG: Gibbs energy change (kJ mol^{-1})

$\Delta_C G$: Gibbs energy change for combustion (kJ mol^{-1})

$\Delta_C G_{SOM}$: Gibbs energy change for combustion of the soil organic matter (kJ mol^{-1} C)

$\Delta_r G_{SOM:}$ Gibbs energy change for microbial catabolism of the soil organic matter (kJ mol^{-1} C)

ΔH: Enthalpy change (kJ mol^{-1})

$\Delta_C H^0$: Enthalpy change for combustion at standard conditions (kJ mol^{-1})

$\Delta_C H_{SOM}$: Enthalpy change for combustion of SOM (kJ mol^{-1} C)

$\Delta_r H_{SOM}$: Enthalpy change for microbial catabolism of the soil organic matter (kJ mol^{-1} C)

Q_o : Oxycaloric quotient (kJ / Cmol /degree of reduction)

Q_{SOM}: Heat of combustion of SOM (kJ g^{-1} SOM)

R_{CO2}: Rate of CO_2 release by soil organic matter microbial catabolism in micromol of CO_2 per gram of soil and hour (µmol CO_2-C g^{-1} h^{-1})

R_q: Heat rate of soil organic matter microbial catabolism in millijoules per gram of soil and hour (mJ $g^{-1}h^{-1}$)

ΔS: Entropy change (J mol^{-1} K^{-1})

$\Delta_C S_{SOM}$: Entropy change for the combustion of the soil organic matter (J mol^{-1}C K^{-1}).

$\Delta_r S_{SOM}$: Entropy change for the microbial catabolism of the soil organic matter (J mol^{-1}C K^{-1})

SOM: Soil organic matter

γ_C: Degree of reduction of the soil organic matter

γ_r: Degree of reduction of the substrates from SOM being metabolized by soil microorganisms

Introduction

Life on earth is subject to the same laws of thermodynamics as inanimate systems. However, application of thermodynamics to living systems has been and still remains as a challenge, being the target of many best-selling books exploring philosophical, ideological, economic, even social and psychological implications of Thermodynamics Laws (Schrödinger 1944, Odum 1969, Prigogine et al. 1972, Corning 2005). Application of thermodynamics to living systems leads to understanding of the mechanisms they utilize to manage their energy, as well as, to the capacity of all these systems to survive on earth. These questions have been largely discussed under a thermodynamic perspective during the last century (Schrödinger 1944, Odum 1969, Prigogine et al. 1972), and still continue because of difficulties in calculating thermodynamic parameters for biological processes (Hansen et al. 2018_a). For this reason thermodynamics of the soil microbial reactions is still an unexplored field, despite literature describing many examples of how thermodynamic laws explain microbial metabolism and microbial growth reactions (Battley 1999, von Stockar et al. 2006, Hansen et al. 2018_a). Attempts to apply these concepts to soil bioprocesses are few and very recent (Barros et al. 2001, Herrmann and Bölscher 2015).

Last advances in understanding the energetics of soil microbial metabolism (Barros et al. 2007, Rong et al. 2007, Hansen et al. 2017), as well as the availability of new calorimeters with new capabilities to measure heat rates from different reactions (Suurkuusk et al. 2017), allows further development of the role of thermodynamics in understanding the soil system.

Soil can be described thermodynamically as an open system interchanging energy and matter with the environment, continuously fed by organic matter supplied from terrestrial ecosystems. Microbiological degradation of the organic input material is

responsible, together with direct oxidation by O_2 and hydrolysis reactions, for the chemical evolution toward mineral soil. The understanding of this evolution is a subject still under development due to the complexity of the soil organic matter, defined now as a "complex bio-organo-mineral system" responsible for soil functionality and soil fertility (Manlay et al. 2007). It underpins human health and survival, being essential for food and fibre production as well as playing an essential role as a carbon sink for mitigating atmospheric carbon emissions. Despite the consequent focus on SOM there is still large uncertainty regarding the mechanisms of the soil formation and the transformation of labile organic matter inputs into relatively stable humus. Soil is an inherently complex material subject to spatial and temporal variability in internal and external properties and drivers that shape its development or degradation. These include soil properties such as texture, mineralogy and organic matter content, as well as external drivers such as land use and land use change, climate (principally precipitation and temperature) and atmospheric deposition. Consequently the cross disciplinary study of SOM is confronted with an enormous number of variables driving the mechanisms leading to soil formation and soil evolution. The concept of soil as an energy source makes thermodynamics an attractive option to explore in order to develop and to understand the role of the energy of SOM on the soil evolution. The first step to this understanding requires determination of the Gibbs energy, enthalpy, and entropy for SOM mineralization to CO_2 and water as a function of the degree of degradation. It involves the measurement of the energy of the organic matter that feeds the microbial population, and the energy of the soil microbial metabolism.

The energy content of the soil organic matter (SOM) can be determined by bomb calorimetry (Jung et al. 1999) or by differential scanning calorimetry (DSC), a routine tool to provide the enthalpy for different materials (Baraldi et al. 1998). Although both methods can fail to capture all of the heat produced during combustion, improvements in DSC technology are yielding heats of combustion values for soils, close to those reported for

organic compounds (Barré et al. 2016, Hansen et al. 2018_b). DSC is thus a rapid way to investigate and to approach to the total enthalpy change for combustion of SOM.

Calorespirometry permits the direct measurement of the heat and CO_2 dissipation rates of any living system including soil (Wadsö and Hansen 2015, Barros et al. 2016) which also yields the enthalpy change for catabolism of SOM at intermediate stages. Consequently, by these two procedures we can monitor the evolution of the soil thermal properties and the soil microbial activity linking the soil energy budget to the rate at which that energy is being dissipated, essential steps to proceed to the development of the thermodynamics of SOM decomposition.

This paper aims to determine and to monitor evolution of the thermodynamic properties of SOM across different soil horizons with the purpose of achieving a deeper understanding of the potential of thermodynamics to describe SOM changes from the surface litter layer to sub-surface mineral soil, as well as to describe the spatial variability of soil properties.

Material and Methods

Sampling sites

The study was conducted at three semi-natural oak woodland sites in south west Ireland. The mean annual rainfall is > 2000 mm and the mean annual temperature is circa 9-10 °*C* (1981-2010 average) (Walsh 2012). The dominant soil type is podzols and while podzols under oak woodland are not common in Europe, they do occur in semi-natural oak woodlandsin Ireland (Little et al. 1990). While semi-natural oakwood was widespread in the past, decades of deforestation cleared such forests on more fertile sites. Those forests which remain are on sites in remote and/or inaccessible locations with relatively poor soils (McCracken 1971). In Ireland, podzols occur in upland regions with relatively high

precipitation and siliceous parent materials (Gardiner and Radford, 1980). They have a peat surface layer (O horizon). This overlies a leached, ash-grey mineral horizon (E horizon). This horizon overlies a yellowish-red B horizon. The C horizon originates as bedrock or glacial till and is very stony.

The sites were chose from a series of 14 sites used by Little et al. (1990). The three sites are Derrycunnihy (491537.228, 580411.229) (DC samples), Glengarriff (492662.632, 556212.602) (G samples) and Uragh (482978.239, 563077.816) (K samples). The site locations can be viewed at: http://map.geohive.ie/mapviewer.html. The parent material at all sites is Devonian sandstone and the dominant soil type is Podzol. The principal tree species are Sessile oak (*Quercus petraea* (Matt.) Liebl.) Downy birch (*Betula pubescens* Ehrh.), Holly (*Ilex aquifolium* L.) and Rowan (So*rbus aucuparia* L.) with ground vegetation consisting of Bilberry (*Vaccinium myrtillis* L.), Greater wood-rush (*Luzula sylvatica* (Huds.) Gaud.) and Heather (*Calluna vulgaris* (L.) Hull). Examination of historical maps by Little et al. (1990) suggested that all sites carried deciduous woodland as recently as 1840.

Soil sampling

Field work was conducted in August 2016. At each study site, between three and five sampling points were identified with each point located mid-way between the tree stem and the maximum crown radius of a Sessile oak tree. Firstly, a rectangular quadrat of 0.25 × 0.25 m was used to collect all loose litter (*L*) and fermented (*F*) layer within the quadrat at each sampling point. Thereafter, using a hammering head and stainless steel rings of 100 cm^3 volume (Eijkelkamp Soil and Water B.V., The Netherlands), bulk density (*BD*) samples of the humic (*H*) layer was collected. After removing the entire *H* layer, the same process was used to collect one *BD* sample of the top 5 cm of the mineral layer (*M* samples). In addition, three extra cores were taken at each location for further chemical, thermal and calorespirometric analysis. Within each stand, samples from the five locations

were mixed together and bulked samples were prepared for all laboratory analysis. In all cases, depth of the different *L/F*, *H* and *M* layers were recorded and sampling produced minimum disturbance and compaction. In some cases, the shallowness of the *H* layer and the abundance of stones prevented the collection of *BD* samples from the *H* and *M* profile, respectively.

Soil samples taken for the determination of *BD* were broken up manually, spread on plastic trays and air dried for 48 hours. Thereafter, coarse fractions (i.e. plant material and stones) greater than 2mm were set aside and remaining sample was ground using a 2-mm sieve in a rotor mill to separate fine and coarse soil fractions. Both fractions were then oven-dried at 105*ºC* for 24 hours (or until constant weight) and their mass (±0.01 g) was recorded. The water displacement method was used to measure the volume of the coarse fraction. The difference between the volumes of the *BD* ring and the coarse fraction represented the volume of the fine earth fraction (Clancy et al. 2015). Bulk density was calculated by dividing the oven dry mass by the volume of the density rings. In addition, *BD* of the fine earth fraction was also calculated by dividing the oven dry mass of the fine earth fraction by the corrected volume in each case.

Samples for thermal analysis were air dried at laboratory temperature. *L/F* and *H* samples were ground and the mineral samples were sieved through 2 mm.

Samples for calorespirometric measurements were kept at the humidity they had after sampling and mineral samples sieved at 2 mm too. Then, about 100 gram from each sampling site and horizons were kept in separated polyethylene bags and frozen at -21 *ºC* until the moment of the measurements.

Thermal analysis

Thermal properties of the samples were studied by thermogravimetry (*TG*) (*TGA-DSC1* Mettler Toledo). For *TG* analysis, samples were placed in 100 µL open aluminium pans under a dry air flow of 50 mL min^{-1} with a temperature ramp from 50 to 600 *ºC* at 10 *ºC* min^{-1}.

DTG curves (first derivative of *TG* traces) indicate the resistance of SOM to thermal oxidation in air. *TG* traces determine the quantity of SOM fractions with different resistance to oxidation as defined by the temperatures at the maxima of the different combustion peaks in the *DTG* curves. In this paper *DTG* curves were used to determine the organic matter content of the samples, SOM, defined as the mass loss between 180 ºC and 600 ºC divided by the mass of the sample, the SOM thermal fractions, the percentage of char after combustion and the *T50-TG*, that is the temperature at which 50 % of the organic matter is combusted.

DSC shows the profile of the energy released by combustion of the SOM. The quantity of energy from SOM is determined by integration of the *DSC* curves versus time after base line correction. This heat quantity needs to be normalized to the SOM content of the samples given by the *TG*, in order to obtain the total energy content of SOM, Q_{SOM}, in kilojoules per g of soil organic matter (kJ / g SOM). To obtain the enthalpy of combustion, $\Delta_c H_{SOM}$ at 25 ºC, 1.839 kJ / g SOM was added to Q_{SOM} (Baraldi et al. 1998) and then converted to C mol. *DSC* curves were also used to determine the *T50-DSC* of the samples, the temperature at which 50 % of the SOM energy content is released during the combustion. Both, *T50-TG* and *T50-DSC* are indices of thermal stability.

Isotope ratio mass spectrometry (*IRMS*)

Stable *C* isotope analyses at natural abundance levels were carried out to determine the $\delta^{13}C$ signature ($^{13}C/^{12}C$ ratio) at two different soil depths: the mineral soil layer (*M* samples) and the organic-rich topsoil layer (*L/F* samples), using a Finnigan MAT Delta C isotope-ratio mass spectrometer (Finnigan MAT, Bremen, Germany) coupled to a Carlo Erba CNS 1508 elemental analyzer (Carlo Erba Instruments, Milan, Italy). The $^{13}C/^{12}C$ ratio was determined not only along the edaphic profile but also at the end of the calorespirometric measurements in the *L/F* soil layer, in order to quantify possible isotopic changes along the SOM biodegradative process caused by the soil microbial metabolism when samples were placed in the calorimeter. The $^{13}C/^{12}C$ ratio of soil or litter samples was expressed as $\delta^{13}C$ signature according to the following equation, which is based on the deviation of the $^{13}C/^{12}C$ ratio from the reference standard (VPDB, Vienna Pee Dee Belemnite), where $R = {}^{13}C/^{12}C$:

$$\delta^{13}C\ (‰) = (R_{sample}/R_{standard} - 1) \times 10^3 \qquad (1)$$

As part of each analytical batch run, a set of international reference materials (NBS 22, IAEA-CH-6, USGS 24) was analyzed. The precision (standard deviation) for the analysis of $\delta^{13}C$ of the laboratory standard (acetanilide) was lower than ± 0.15‰ (n=10).

Calorespirometry

Calorespirometric measurements were done with a six channel TAM III calorimeter (TA Instruments, Lindon, UT). In each calorimetric measurement, six aliquots of 0.600 g (for *L/F* samples) to 1 g (*H* and *M* samples) each from a 20 - 10 g thawed samples, were sealed in 4 ml stainless steel ampoules and placed in the calorimeter. Prior to these measurements, defreeze was monitored by calorimetry. Thawing and rewetting of samples to bring soil to the same water content can cause fluxes of heat and CO_2 due to soil

disturbance that may distort the calorespirometric measurements. For this reason, they were done once samples reached the necessary steady metabolic state activated after thawing and after rewetting samples to 60 % of their water holding capacity (WHC). This stabilization prior to the measurements was monitored by calorimetry to determine the time needed by each sample to reach a steady metabolic state after the perturbation had ended. The time needed was similar for the *H* and *M* samples (about two weeks) and shorter in the *L/F* samples (about 10 days). After stabilization of samples, a small vial with 0.4 M NaOH was introduced into three of the ampoules (one for each sample) to measure the sum of the metabolic heat and CO_2 rates for each of the soil layers analyzed. Measurements were done at 25 *ºC* at isothermal conditions. The procedure for the simultaneous measurements of heat and CO_2 is explained in detail in previous reports (Barros 2018). Calorespirometric measurement with 6 ampoules takes 48 hours for *H* and *M* samples, and about 24 hours for *L/F* samples, before inhibition due to oxygen depletion takes place, yielding duplicates of the CO_2 and heat rates in all cases (n=2 ± SD) for each soil. The measured rates were averaged over a 22 hour time period excluding the initial equilibration period, by integrating the heat and CO_2 rates over the same time period of about 22 hours, to give the heat rate, R_q, in millijoules per gram of soil and hour, (mJ / g h) and the CO_2 rate, R_{CO2}, in micromole CO_2 per gram of soil and hour (µmol CO_2/g h). Then, R_q can be divided by the R_{CO2} to obtain the calorespirometric ratio (*CR*) of the soil microbial metabolism in kilojoules per mol of CO_2 (kJ/mol CO_2).

Statistical analysis

Comparison of thermodynamic parameters obtained by independent methods was done by one way ANOVA (n=9, $p< 0.05$) after checking normality and homoscedasticity of data by Shapiro-Wills and Levene´s test respectively. Comparison of SOM properties and biodegradation rates among sites were done by averaged data and standard deviation (n =

2 ± sd). Pearson´s correlation was applied to study the relation among SOM properties, biodegradability and thermodynamic parameters. Contribution of all these parameters to the variance among sites was studied by multivariate analysis, more specifically by principal components analysis (PCA).

Thermodynamic theory

The enthalpy of combustion of SOM to CO_2 and water, $\Delta_c H_{SOM}$, can be approached by DSC where the combustion of SOM can be written as follows:

$$SOM(s) + xO_2(g) \rightarrow yCO_2(g) + H_2O(g) \qquad \Delta_c H_{SOM} \qquad (2)$$

Once $\Delta_c H_{SOM}$ is obtained, the degree of reduction of carbon in SOM, γ_C, can be determined by the following equation (Thornton 1917, Patel and Erickson 1981, Cordier et al. 1987):

$$\Delta_c H^0 = Q_o \, \gamma_C \qquad (3)$$

Where $\Delta_c H^0$ is the enthalpy of combustion of organic substrates and Q_0 the oxycaloric quotient representing the ratio between the enthalpy of combustion and the degree of reduction for organic compounds. Q_0 has been adapted for a large number of organic substrates, as well as for their decomposing reactions. Here, we used the value of -109 kJ / Cmol/degree of reduction, obtained from the average of the heat of combustion of a large set of organic compounds in the pure, dry state (Sandler and Orbey 1991). It is also the value applied for calculation of degree of reduction of carbon in dried organic materials derived for plants (Gary et al. 1995). Therefore, equation (3) is applied to equation (2) for soil samples to calculate γ_C as follows:

$$\gamma_C = \Delta_c H_{SOM} \text{ / -109 kJ/Cmol/degree of reduction} \qquad (4)$$

267 γ_C in equation (4) represents the degree of reduction of carbon from SOM. $\Delta_c H_{SOM}$
268 denotes the energy stored by the entire SOM macromolecule and the source of energy for
269 soil microorganisms.

270 A similar relation exists for estimating the Gibbs energy change for combustion of
271 dry organic materials (Sandler and Orbey 1991):

272 $\Delta_c G = \gamma_C$ (-110.23 kJ/Cmol/degree of reduction) (5)

273 Therefore, γ_C obtained by equation (4) also allows calculation of the Gibbs energy
274 change, $\Delta_c G_{SOM}$, for combustion of SOM in equation (2). $\Delta_c G_{SOM}$ is the existing driven force
275 in soil for microbial metabolism.

276 $\Delta_c H_{SOM}$ and $\Delta_c G_{SOM}$ must be normalized to the soil C content in order to apply
277 equations 4 and 5. The conversion factor used was the relation between the C and SOM
278 percentages of samples.

279 Calorespirometry permits simultaneous measurement of the heat and CO_2
280 dissipation rates from soil microbial metabolism (Barros et al. 2011, Wadsö and Hansen
281 2015, Herrmann and Bölscher 2015). The quotient between the heat and CO_2 rate, R_q/RCO_2
282 is the calorespirometric ratio of the microbial metabolism, a measure of the enthalpy
283 change of microbial catabolism of SOM, $\Delta_r H_{SOM}$, when is determined at microbial basal or
284 maintenance metabolism (Hansen et al. 2004, Barros et al. 2016). At these conditions SOM
285 biodecomposition can be written as follows:

286 $SOM(s) + xO_2(g) \rightarrow yCO_2(g) + H_2O(l)$ $\Delta_r H_{SOM}$ (6)

287 The calorespirometric ratios determined for equation (6) yield the degree of
288 reduction of the substrate being metabolized by soil microorganisms, γ_r, by the following
289 equation adapted for soils (Battley 1999, Hansen et al. 2004):

290 $R_q/R_{CO2} \approx \Delta_r H_{SOM} = \gamma_r/4(-455)$ kJ/molO_2 (7)

291 The multiplier $\gamma_r/4$ is the ratio of moles of O_2 to moles of CO_2 and -455 kJ / mol O_2
292 is the reported oxycaloric equivalent for aerobic metabolism (Gnaiger and Kemp 1990,
293 Maskow et al. 2010). It usually represents 80% of the total microbial metabolism in soils.

294 Once the degree of reduction of substrates from SOM being metabolized is known,
295 the Gibbs energy change for equation (6) can be determined by the following relation
296 adapted for microbial decomposition of organic substrates yielding liquid water and CO_2 in
297 an aqueous solution (Roels 1983):

298 $\Delta_r G_{SOM}$ = -86.6 - γ_r (94.4 kJ/Cmol/degree of reduction) (8)

299 Where $\Delta_r G_{SOM}$ is the Gibbs energy change of the substrates being metabolized by
300 microorganisms.

301 Microbial reactions in the different organic layers constitute an irreversible process.
302 As such, the Gibbs free energy change of those processes is also given by:

303 $\Delta G = \Delta H - T\Delta S$ (9)

304 Where ΔG is the Gibbs energy change of any reaction, ΔH is the enthalpy change of the
305 reaction, T is the temperature and ΔS the entropy change. Equation (9) allows calculation
306 of ΔS for the equations (2) and (6). Note that in the case of reactions in aqueous solution,
307 which is the case for microbial catabolism, $T\Delta S$ is positive and contributes significantly more
308 to ΔG for reaction 6 in aqueous solution than in the dry state (equation 2).

309 Therefore, the triad of thermodynamics, i.e. $\Delta_C H_{SOM}$, $\Delta_C G_{SOM}$, and $\Delta_C S_{SOM}$, for the
310 complete mineralization of SOM to CO_2 and vapor water can be determined from the heat
311 of combustion measurements by DSC. Values for $\Delta_r H_{SOM}$, $\Delta_r G_{SOM}$, and $\Delta_r S_{SOM}$ for
312 mineralization of the portions of SOM being catabolized at a given point in the degradation

process are determined from the calorespirometric measurements of metabolic heat and CO_2 rates, R_q and R_{CO2}.

By this way, the Gibbs energy that microorganisms would dissipate if SOM is entirely metabolized as a continuum ($\Delta_c G_{SOM}$), can be compared to the Gibbs energy of the substrate being metabolized during the calorimetric measurement ($\Delta_r G_{SOM}$) given by the experimental values of calorespirometric ratios.

Results

Elemental composition, $\delta^{13}C$ data and bulk density properties

SOM together with *C* percentages, $\delta^{13}C$ values and *BD* of samples are shown in table 1. S*OM* and *C* percentages deplete from *L/F* to mineral soils with apparently no differences among sites in the *L/F* layers and higher variability in the *H* and *M* layers.

$\delta^{13}C$ data from the three sites are in the range of values typical of C_3 vegetation ecosystems (Cabaneiro and Fernandez 2015, Fernandez et al. 2012), but show differences between the L/F and M layers with $\delta^{13}C$ enrichment with increasing depth, attributed to mineralization and humification processes of SOM (Nadelhoffer and Fry 1988, Fernandez et al. 2003).

As expected, the bulk density, BD, increases with depth as the low density organic material is replaced with mineral silicate matter. The higher microbial respiratory activity linked to lower bulk density (Fraser et al. 2016) is thus likely the result of increasing the SOM fraction.

SOM Thermal properties

Figure 1 shows the *DSC* and *DTG* curves of the samples. *L/F* and *H* horizons show a similar profile of bimodal curves with maximum peak temperatures varying from 314 *ºC* to

335 ºC in the *L/F* samples, and 303-305 ºC in the *H* samples. Temperatures of the second peak were 415-428 ºC in the *L/F* samples and 417-424 ºC in the *H* samples. *DSC* and *DTG* curves from the *L/F* and *H* horizons are typical for lignocellulosic material and do not show much variability among the three different sampling sites. Mineral soils show a different profile of the DSC and DTG curves suggesting changes in the SOM nature compared to those from the upper soil organic layers. Temperatures of both combustion peaks tend to decrease from the *L/F* horizon to the mineral soil.

DTG curves give the SOM thermal fractions associated to each of the combustion peaks, yielding two fractions with different thermal stability, called *Exo1* and *Exo2* (Figure 2). SOM thermal composition of *L/F* samples is similar among sites. All of them have higher *Exo1* than *Exo2* fractions and low char percentages (0.18 to 0.50 %). The *Exo 1* fraction decreased in the *H* horizons, except in the *G* samples, and the char percentages increase in all cases. All *M* samples have similar *Exo1* and *Exo2* percentages and the highest char content of all layers. Therefore, as we dig deeper in soil, the labile SOM fraction (*Exo1*) decreases until it equals the *Exo2* fraction and the char content increases. $\delta^{13}C$ is closely positively correlated with char ($r^2 = 0.90$; $p < 0.005$).

Parameters linked to thermal stability (*T50-DSC* and *T50-TG,* Table 1) show no clear trend but all mineral samples are less thermally stable than the *L/F* ones.

$\Delta_c H_{SOM}$ is similar among sampling sites but shows a clear trend to increase from *L/F* to mineral samples indicating changes in the SOM nature (Table 1). Assuming that $\Delta_c H_{SOM}$ measures the energy budget of the soil organic substrates used by the microbial population, equation 4 can be applied to determine the degree of reduction of SOM, γ_C, also shown in table 1. All *L/F* samples have γ_C values close to those of carbohydrates ($\gamma_C = 4$) and tend to increase from the top soil layer to the mineral samples where values show SOM more reduced than carbohydrates, approaching to values reported for lignocellulosic

361 material and lignin in some of the *H* and *M* samples (Gary et al. 1995, Voitkevich et al.
362 2012). Therefore, the degree of reduction of SOM in the mineral soils is higher than those in
363 the surface organic layers with little variability among sampling sites for the *L/F* layer, and
364 more spatial variability in the *H* and *M* soils. The degree of reductance of SOM in the
365 mineral soils followed the order Derrycunnihy (*DCM*) > Glengarriff (*GM*) > Uragh (*KM*).

366 Values obtained for $\Delta_c G_{SOM}$ by equation 5 are shown in table 1 too, as well as the
367 entropy change of equation 2, $\Delta_c S_{SOM}$.

368 **Microbial activity**

369 R_{CO2} and R_q values (CO_2 and heat rates respectively) were in all cases similar among
370 sites and showed a clear trend to decrease from the *L/F* layers to the mineral soil (Figure 3).
371 R_q and R_{CO2} rates were positively correlated to the Exo1 percentages of samples (n = 9; r^2 =
372 0.60 $p < 0.01$; $r^2 = 0.53$ $p < 0.05$ respectively) and negatively correlated to the Q_{SOM} (r^2 =
373 0.53 $p < 0.05$ for R_q, $r^2 = 0.49$ $p < 0.05$ for R_{CO2}) reflecting depletion of rates with increased
374 degree of reductance of SOM. R_q, R_{CO2} and $\delta^{13}C$ are negatively correlated too (r^2 = - 0.95; p <
375 0.001; r^2 = -0.90, p< 0.005 respectively).

376 The enthalpy changes, $\Delta_r H_{SOM}$, calculated as the ratio R_q/R_{CO2} are given in table 1.
377 The magnitude of the $\Delta_r H_{SOM}$ values increases from the L/F samples to the H and M
378 samples, and in all cases, except DCH, are less exothermic than corresponding $\Delta_C H_{SOM}$
379 values. This clearly indicates that microbial catabolism is oxidizing only a more oxidized
380 fraction of the total SOM. ANOVA shows γ_r and γ_C are significantly different (n = 9, $p < 0.05$).
381 The $\Delta_r H_{SOM}$ values for the L/F samples are less negative than their heat of combustion,
382 $\Delta_C H_{SOM}$, indicating the substrates of catabolism are more oxidized than carbohydrates. The
383 $\Delta_r H_{SOM}$ values for the H and M samples indicate the substrate being used in catabolism is
384 carbohydrate, likely cellulose, with γ_r close to 4. The data show catabolism transforms SOM
385 from a state of lower energy per Cmole, but easily and rapidly metabolized materials such

386 as sugars and hemicellulose, to a state with higher energy per Cmole, but difficult to
387 metabolize materials such as lignocellulose requiring specialized enzymes to break it down
388 into small, soluble molecules.

389 When the relation between $\Delta_r H_{SOM}$ and $\Delta_c H_{SOM}$ is given by the ratio $\Delta_r H_{SOM}$ / $\Delta_c H_{SOM}$
390 similarly to the ratios suggested by common orientors for soil ecological evolution (Ludovisi
391 et al. 2005), it is obtained that ratio varies from 1.11 to 0.62 among samples (Table 1). That
392 is the fraction of the energy from the total soil energy budget being used by
393 microorganisms.

394 Values for $\Delta_r G_{SOM}$ obtained by equation (8) can be seen in table 1. Although $\Delta_r G_{SOM}$
395 is less negative than $\Delta_c G_{SOM}$, ANOVA yielded differences between both values were not
396 significant ($n = 9$; $p < 0.05$). The entropy change for the microbial reaction, $\Delta_r S_{SOM}$, is
397 significantly higher than the entropy change for the combustion reaction in the DSC, $\Delta_c S_{SOM}$.
398 $\Delta_c S_{SOM}$ changes little across the samples while $\Delta_r S_{SOM}$ decreases from the L/F layer to the H
399 layer and M layers and is negatively correlated with $\Delta_r H_{SOM}$ ($r^2 = 0.99$; $p < 0.001$). The
400 correlation between $\Delta_c S_{SOM}$ and $\Delta_c H_{SOM}$ is positive and weaker ($r^2 = 0.76$; $p < 0.01$).

401 To determine the main factors influencing the energetics of SOM decomposition
402 and to obtain a more integrated understanding of the thermodynamic behaviour observed
403 in the different edaphic samples, the overall variance of all the calculated parameters
404 among samples from different sites and/or soil depths was examined by means of
405 multivariate analysis. Thus, PCA was initially applied to a data matrix composed by all
406 examined variables concerning SOM chemical and thermal composition, biodegradability,
407 and thermodynamic properties, by taking into account the whole dataset corresponding to
408 the 9 different soil samples collected from the 3 studied sites (3 corresponding to *L/F* layer,
409 plus 3 to *H* layer, plus 3 to *M* layer). This initial PCA approach yields two principal
410 components (PC1, PC2) that explain more than 83 % of the total dataset variability (56.7 %

411 and 26.8 % for PC1 and PC2, respectively). Results are shown in figure S1 as supplementary
412 material. The PC1 was mainly defined by microbial degradation rates (R_q and R_{CO2}), degree
413 of reduction of substrates being metabolized (γ_r) and by the thermodynamic parameters
414 obtained for SOM catabolism ($\Delta_r H_{SOM}$, $\Delta_r G_{SOM}$ and $\Delta_r S_{SOM}$), while the largest contributions to
415 PC2 comes from variables linked to the SOM content (C), SOM thermal fractions (*Exo1*,
416 *Exo2* and char) and thermal properties (*T50-TG* and *T50-DSC*). Thermodynamic parameters
417 linked to SOM combustion properties showed the lowest contribution to both PC1 and PC2.
418 Therefore, these results point to thermodynamics of the microbial decomposition of SOM
419 as the main source of variability among these soil samples, followed by the SOM elemental
420 and thermal properties.

421 In order to better focus the statistical analysis on the thermal and thermodynamic
422 properties of SOM exclusively, a new PCA was done with only 9 indices representing the
423 direct thermal and thermodynamic properties of SOM: SOM thermal fractions (Exo1, Exo2
424 and char), SOM microbial degradation rates (R_q and R_{CO2}) and thermodynamic indices
425 ($\Delta_C H_{SOM}$, $\Delta_r H_{SOM}$, $\Delta_C S_{SOM}$, $\Delta_r S_{SOM}$). This targeted selection showed up two PC components
426 explaining 86 % of the total variance (Figure 4). The enthalpy and entropy change of the
427 microbial SOM catabolism ($\Delta_r H_{SOM}$, $\Delta_r S_{SOM}$) together with the microbial degradation rates (R_q
428 and R_{CO2}) continue with the largest contribution to PC1 (66.3 %). Soil thermal fractions have
429 the highest contribution to PC2 (19.9 %) while the enthalpy and entropy change of SOM
430 combustion ($\Delta_C H_{SOM}$ and $\Delta_C S_{SOM}$) continue to be the indices with less contribution to the
431 total variance among samples.

432 Figure 4 shows the distribution of the soil samples with regards to the first 2 principal
433 components, PC1 *vs* PC2. Their location on this two-dimensional subspace allows sample
434 differentiation according to their particular SOM characteristics. The grouping of samples
435 seems to depend on their specific vertical location within the soil profile. Samples from the

436 *L/F* layer (with quite homogeneous features among the different sampling sites) were
437 closely located in the positive arm of PC1 due to their higher CO_2 rates, heat rates and
438 $\Delta_r S_{SOM}$. In contrast, soil samples from the mineral layer (that exhibited more heterogeneous
439 characteristics among sampling sites and higher spatial variability) were more scattered
440 through the PCA representation, being the only ones located in the negative arm of PC2,
441 mainly due to their relatively high char content. H samples were the ones more dispersed
442 along the bi-plot. All H samples studied, with higher Exo1 or Exo2 fractions but lower
443 microbial degradation rates than samples from the *L/F* layer, were the only ones which
444 location was always within the second quadrant of the graph. These results confirm how
445 spatial variability concerning SOM properties and bio-decomposition increases as we dig
446 deeper into the soil profile and as SOM becomes more transformed by microbial action.

447 **Discussion**

448 Results in this work verify how thermal analysis and calorimetry directly and
449 indirectly can connect SOM properties with SOM biodegradability as a way to asses SOM
450 recalcitrance, microbial strategies of SOM biodegradation and the possible role of
451 thermodynamics on them. In spite of several attempts involving only mineral soil samples
452 (Peltre et al. 2013, Kucerik and Siewert 2014), it is not always possible to correlate SOM
453 thermal properties to biodegradability at the conditions reported by the literature, because
454 when working with mineral soils, thermal properties are affected by factors like *C* content,
455 C/N ratio and clay content which may interfere in the correlation with the biological activity
456 (Plante et al. 2005, Kucerik et al. 2018). Nevertheless, thermal analysis data about the
457 vertical evolution of SOM along the different soil organic layers seems to reflect quite well
458 SOM evolution to a more recalcitrant state. This increased recalcitrance is assumed here by
459 the increment of $\Delta_C H_{SOM}$ accompanied by the depletion of the heat and CO_2 rates, increases
460 in char content, in *BD* and $\delta^{13}C$ enrichments at greater depths. $\Delta_C H_{SOM}$ has been rarely used

as a SOM property due to technological reasons, but new *DSC* devices can measure simultaneously the energy and mass losses, improving accuracy and yielding Q_{SOM} values close to the heat of combustion of organic material reported by the literature (Gary et al. 1995, Villanueva et al. 2011, Voitkevich et al. 2012) and to values from mineral soils reported recently (Berre et al. 2016, Barros et al. 2016, Barros 2018). Calculation of $\Delta_C H_{SOM}$ yields the possibility to quantify SOM recalcitrance by the degree of reduction, γ_C. Values obtained for the *L/F* layers where the organic material is slightly degraded indicate a degree of reduction similar to the carbohydrates, the main component of the litter for Oak trees (Chávez-Bergara et al. 2014). The litter from oak trees becomes more aromatic (more lignaceous and phenolic) as decomposition proceeds (Chávez-Bergara et al. 2014) which agrees with the increasing exothermicity of $\Delta_C H_{SOM}$ with depth seen here.

By the calculation of the $\Delta_r H_{SOM}$ and $\Delta_C H_{SOM}$, it is suggested the ratio $\Delta_r H_{SOM}$ / $\Delta_C H_{SOM}$, to quantify the extent at which the microbial community uses the soil energy budget given by the $\Delta_C H_{SOM}$. This ratio could act as a thermodynamic orientor (Ludovisi et al. 2005) to forecast changes within a soil ecosystem. The theory is that if these ratios approach at 1, succession occurs (Odum, 1969, Choi et al., 1999). Values obtained here show the substrates that microbial population use from SOM involves about 80 % of the total energy in SOM. It would be worthy to explore how these values evolve with soil ecosystems at different degree of maturity.

The $\Delta_C H_{SOM}$ and the $\Delta_r H_{SOM}$ obtained by direct measurements have the advantage to allow calculation of the free energy and entropy changes for each of the soil horizons. $\Delta_C G_{SOM}$ values determined for the different soil layers are close to those reported for glucose (ΔG = -474 kJ /Cmol), for cellulose (ΔG = -504 kJ/Cmol) and lignin material (ΔG = -556 kJ/Cmol) (Voitkevich et al. 2012, Goldberg et al. 2015). $\Delta_C S_{SOM}$, along the different soil layers varied between 13.42 and 26.85 J/K C mol. $\Delta_C S_{SOM}$ contributes little to $\Delta_C G_{SOM}$ and to

variance among samples as shown by PCA (Figure 4). On the opposite, the microbial decomposition of SOM is responsible for most of the variance among samples, and the main source of entropy changes, as observed with $\Delta_r S_{SOM}$ values (von Stockar et al. 1993, von Stockar and Liu 1999). It is assumed that the entropy change should increase with higher degree of reduction of organic substrates (Roels 1983) as happens with the observed evolution of $\Delta_C S_{SOM}$ but $\Delta_r S_{SOM}$ values decreased as SOM turned more reduced. This is still difficult to explain for the soil microbial metabolism and will need more exploration with more soil ecosystems. A possible explanation could be $\Delta_r S_{SOM}$ be sensitive to changes in the microbial structure through the different soil layers. The observed microbial adaptation to SOM evolution could be explained in the light of the r-K concept (MacArthur and Wilson, 1967) that identifies two main opposite ecological strategies: the r-strategy characterized by high reproduction rates, small size and low life time, that would prevail or would be fed by the thermodynamic conditions of L/F and H layers, involving higher positive metabolic entropy, and the K-strategies, followed by species characterized by larger size and lower rates (high turnover times) prevailing in the later stages of development, that could be favored by similar thermodynamic conditions to those found in the mineral samples. Evolution of $\Delta_r S_{SOM}$ could be reflecting these changes in the microbial structure and functions through the different soil horizons.

The results of this work on the thermodynamics of evolution of SOM from L/F topsoil to mineral soil support the soil continuum model (SCM) (Lehmann and Kleber 2005). That is, the initial SOM in the L/F layer evolves to a greater degree of reduction with more kinetically stable macromolecules by metabolism of organic fractions from the SOM with a lesser degree of reduction and lower energy content per Cmole. As the evolution of Exo1 and Exo2 soil thermal fractions suggests, the process begins by decomposing the most kinetically labile SOM fractions in the L/F and H layers, i.e. hemicellulose and cellulose, leaving behind lignin to be transformed later into aromatic products, humic, and fulvic

512 acids. However, our results contradict SCM, in that the end result is SOM at a greater
513 degree of reduction than plant litter. This last can be just a consequence of tracking SOM
514 evolution with mineral soils at lower degree of biodegradation or transformation than the
515 ones reported by the literature as mature soil ecosystems (Barré et al. 2016, Lehmann and
516 Kleber 2005). The degree of reduction, as determined in this study, could be explored as a
517 way to settle the maturity of SOM and therefore, eliminate confusion in defining the
518 maturity of soil ecosystems.

519 The observed variability of the metabolic entropy values may be explained by the
520 SCM too, since it assumes a vast portfolio of options for variations in carbon turnover
521 dynamics affecting the metabolic entropy change (Lehmann and Kleber 2015). It is well
522 known that soil from forest ecosystems such as oak forest, present geographical variations
523 of different SOM properties attached to different environmental and tree characteristics
524 (Cornwell et al. 2008, Pietsch et al. 2018). Therefore, thermodynamic properties of SOM
525 microbial decomposition may be sensitive to all those factors too, being differences among
526 sites more noticeable as the degree of SOM decomposition and SOM transformation
527 increases, as PCA analysis showed up.

528 What it seems to be a general trend is that microorganisms degrade single
529 substrates from the total SOM macromolecule, as a strategy to achieve low dissipative
530 metabolic levels that would help to keep the remaining carbon in the mineral soil. This
531 ability of the soil microbial structure to change fast the type of substrate they metabolized
532 is reflected in the variability of the calorespirometric ratios (linked to $\Delta_r H_{SOM}$ in this paper)
533 (Barros et al. 2011, Barros et al. 2017) but commonly and erroneously interpreted as lack of
534 reproducibility. Similar results have been found when applying calorespirometric ratios to
535 different ecosystems reflecting young and mature states, showing how they tend to
536 decrease in mature sites (Herrmann and Bölscher 2015, Barros et al. 2016) where SOM was
537 more chemically and thermally stable. The main goal of this strategy would be the

preservation of energy within the soil system in spite of the high C losses that SOM transformation involves too, and should reflect the microbial tactic to keep their microbial structure far from the thermodynamic equilibrium (depletion of Gibbs energy).

Results show proofs of concepts revealing the proposed procedures as alternative tools to continue advancing into the thermodynamics of soil systems, as well as initial approaches to develop the thermodynamics of the reactions involved in the soil C cycle, in order to understand the role of microbial bioenergetics on the survival strategies of soil ecosystems.

Declarations

- Acknowledgements- Authors would like to thank the use of RIAIDT-USC analytical facilities for the calorespirometric and thermogravimetric analysis by Dr Verónica Piñeiro and Montserrat Gómez. Authors thank too, Ana Argibay Noal for technical assistance in soil sample preparation for isotopic analysis and the IIAG-CSIC for providing the necessary infrastructure and experimental facilities to perform this work.

- Funding- Although the author's research group received no specific funding for this work, the IIAG-CSIC research group "Ciclo biogeoquímico del carbono edáfico - CibiCed" was partially funded by the "Consellería de Economía, Emprego e Industria" of the Galician Government (OTR02794/AGI/CISIC I+D+I 2016, OTR04174/AGI/CISIC I+D+I 2017). The funders had no role in study design, data collection and analysis, decision to publish, or preparation of the manuscript.

- Author contributions- All authors have equally contributed to the development of this work.

- Conflicts of interest- There are not conflict of interest.

562 **References**

563 Baraldi, P. et al. 1998. Measurements of combustion enthalpies of solids by DSC. – Mater.
564 Chem. Phys. 53: 252-255.

565 Barré, P. et al. 2016. The energetic and chemical signatures of persistent soil organic
566 matter.- Biogeochemistry letters 130: 1-12.

567 Barros, N. et al. 2001. Interpretation of the metabolic enthalpy change, ΔHmet, calculated
568 for microbial growth reactions in soils.- J. Thermal. Anal. Cal. 63: 577-588.

569 Barros, N. et al. 2007. Calorimetry and Soil.-Thermochim. Acta 458: 11-17.

570 Barros, N. et al. 2011. Calorimetric determination of metabolic heat, CO_2 rates, and the
571 calorespirometric ratio of soil basal metabolism.- Geoderma 160: 542-547.
572 Barros, N. et al. 2016. Factors influencing the calorespirometric ratios of soil microbial
573 metabolism.- Soil. Biol. Biochem 92: 221-229.

574 Barros, N. et al. 2017. Effect of soil storage at 4 ºC on the calorespirometric measurements
575 of soil microbial metabolism.- AIMS Microbiol. 3: 762-773.
576 Barros, N. 2018. Calorimetry and Soil Biodegradation: Experimental procedures and
577 thermodynamic models.- In: Bidoia, E.D. and Montagnolli, R.N.(ed.), Toxicity and
578 Biodegradation testing. Humana Press. Springer protocols, pp. 123-145.

579 Battley, E. H. 1999. An empirical method for estimating the entropy of formation and the
580 absolute entropy of dried microbial biomass for use in studies on the thermodynamics of
581 microbial growth.- Thermochim. Acta 326: 7-15.
582 Cabaneiro, A. and Fernández, I. 2015. Disclosing biome sensitivity to atmospheric changes:
583 Stable C isotope ecophysiological dependencies during photosynthetic CO_2 uptake in

584 Maritime pine and Scots pine ecosystems from southwestern Europe.- Environ. Technol.
585 Innov. 4: 52-61.

586 Chávez-Vergara, B. 2014. Organic matter dynamics and microbial activity during
587 decomposition of forest floor under two native neotropical oak species in a temperate
588 deciduous forest in Mexico. - Geoderma. 235-236: 133-145.

589 Choi, J.S. et al. 1999. Measuring perturbation in a complicated thermodynamic world. -Ecol.
590 Model. 117: 143-158.

591 Clancy, M. A. et al. 2015. The need to disaggregate podzols and peaty podzols when
592 assessing forest soil carbon stocks.- Irish Forestry 72(1 & 2): 189-204.

593 Cordier, J. L. et al. 1987. Minireview: the relationship between elemental composition and
594 heat of combustion of microbial biomass.- Appl. Microbiol. Biotechnol 25: 305-312.

595 Corning, P.A. 2005. Holistic Darwinism: Synergy, Cybernetics and Bioeconomics of
596 Evolution.- The University of Chicago Press.
597 Cornwell, W. K. et al. 2008. Plant species traits are the predominant are the predominant
598 control on litter decomposition rates within biomes worldwide.- Ecol. Lett. 11: 1065-1071.

599 Fernandez, I. et al. 2003. Carbon isotopic fractionation during decomposition of plant
600 materials of different quality. -Global Biogeochem. Cy. 17: 1075.

601 Fernandez, I. et al. 2012. Evolution of soil organic matter composition and edaphic carbon
602 effluxes following oak forest clearing for pasture: climate change implications.- Eur. J.
603 Forest Res. 131: 1681-1693.

604 Fraser, F. C. et al. 2016. Distinct respiratory responses of soils to complex organic substrate
605 are governed predominantly by soil architecture and its microbial community.- Soil. Biol.
606 Biochem. 103: 493-501.

607 Gardiner, M.J. and Radford, T. 1980. Soil associations of Ireland and their land use
608 potential: Explanatory bulletin to soil map of Ireland.- Foras Talúntais.

609 Gary, C. et al. 1995. Heat of combustion, degree of reduction and carbon content: 3
610 interrelated methods of estimating the construction cost of plant tissues.- Agronomie 15:
611 59-69.

612 Gnaiger, E. and Kemp, R.B. 1990. Anaerobic metabolism in aerobic mammalian cells:
613 information from the ratio of calorimetric heat flux and respirometric oxygen flux.-Biochim.
614 Biophys. Acta. 1016(3):328-332.
615 Goldberg, R. N. et al. 2015. A thermodynamic investigation of the cellulose allomorphs:
616 Cellulose(am), cellulose Iβ (cr), cellulose II(cr), and cellulose III(cr).- J. Chem.
617 Thermodynamics 81: 184-226.

618 Hansen, L.D. et al. 2004. Use of calorespirometric methods, heat per CO_2 and heat per O_2,
619 to quantify metabolic paths and energetics of growing cells.-Thermochim. Acta 422(1): 55-
620 61.

621 Hansen, L.D. et al. 2017. Biocalorimetry of Plants, Insects, and Soil Microorganisms.- In:
622 Wilhelm, E. and Letcher, T. (ed.), Enthalpy and Internal Energy: Liquids, Solutions and
623 Vapors. Royal Society of Chemistry, pp. 336-363.

624 [a]Hansen, L. D. et al. 2018. Laws of Evolution parallels the Laws of Thermodynamics.- J.
625 Chem. Thermodynamics. 124: 141-148.
626 [b]Hansen, L. D. et al. 2018. Effect of extreme temperatures on soil: A calorimetric approach.
627 – Thermochim. Acta 670: 128-135.

628 Herrmann, A. M. and Bölscher, T. 2015. Simultaneous screening of microbial energetics and
629 CO2 respiration in soil samples from different ecosystems.- Soil. Biol.Biochem. 83: 88-92.

630 Jung, H. J. C. et al. 1999. Accuracy of Klasson Lignin and Acid Detergent Lignin methods as
631 assessed by bomb calorimetry.- J. Agric. Food. Chem 47: 2005-2008.

632 Kucerik, J. and Siewert, C. 2014. Practical application of thermogravimetry in soil science.
633 Part 2: modelling and prediction of soil respiration using thermal mass losses.-J. Thermal.
634 Anal. Cal. 116: 563-570.

635 Kucerik, J. et al. 2018. Linking soil organic matter thermal stability with contents of clay,
636 bound water, organic carbon and nitrogen.- Geoderma 316: 38-46.

637 Lehmann, J. and Kleber, M. 2005. The contentious nature of soil organic matter.- Nature
638 528: 60-68.

639 Little, D. J. et al. 1990. Podzols and associated soils in semi-natural Oak woodlands - A
640 preliminary report.- Irish Forestry, 47(2): 79-89.

641 Ludovisi, A. et al. 2005. The strategy of ecosystem development: specific dissipation as an
642 indicator of ecosystem maturity.- J. Theor. Biol. 235: 33-43.

643 Manlay, R. J. et al. 2007. Historial evolution of soil organic matter concepts and their
644 relationships with the fertility and sustainability of cropping systems.- Agriculture,
645 Ecosystems and Environment 119: 217- 233.

646 Maskow, T. et al. 2010. What heat is telling us about microbial conversions in nature and
647 technology: from chip- to megacalorimetry.-Microbiol. Biotechnol. 3(3):269-284.
648 Mc Arthur, R. H. and Wilson, E. O. 1967. The Theory of Island Biogeography.- Princenton
649 University Press.

650 McCracken, I. 1971. The Irish woods since Tudor Times. - David and Charles, Newton Abbot.
651 Nadelhoffer, K. J. and Fry, B. 1988. Controls on natural nitrogen-15 and carbon-13
652 abundances in forest soil organic matter.- Soil Sci. Soc. Am. J. 52: 1633-1640.

653 Nadelhoffer, K. F. and Fry, B. 1988. Controls on Natural 15N and 13C abundances in forest
654 soil organic matter.- Soil. Sci. Soc. Am. J. 52: 1633-1640.

655 Odum, E. P. 1969. The strategy of Ecosystem Development. – Science 164: 262-270.
656 Patel, S. A. and Erickson, L. E. 1981. Estimation of heat of combustion of biomass from
657 elemental analysis using available electron concepts.- Biotechnol, Bioeng 23: 2051-2067.

658 Peltre, C. et al. 2013. Relationships between biological and thermal indices of soil organic
659 matter stability differ with soil organic carbon level.- Soil. Sci. Soc. Am. J. 77(6): 2020-2028.

660 Pietsch, K. A. et al. 2018. Wood decomposition is more strongly by temperature than by tree species
661 and decomposer diversity in highly species rich subtropical forests.- Oikos doi: 10.1111/oi k
662 .0 4 879.
663 Plante, A.F. et al. 2005. Changes in clay-associated organic matter quality in a C depletion
664 sequence as measured by thermal analyses.- Geoderma 129: 186-199.
665 Prigogine, L. et al. 1972. Thermodynamics of Evolution.- Physics Today 25: 12-38.
666 Roels, J. A. 1983. Energetics and kinetics in biotechnology.- Elsevier Biomedical Press.
667 Rong, X. M. et al. 2007. Isothermal microcalorimetry: A review of applications in soil and
668 environmental sciences.- Pedosphere 17: 137-145.

669 Sandler, S. I. and Orbey, H. 1991. On the thermodynamics of microbial growth processes.-
670 Biotechnol. Bioeng. 38: 697-718.

671 Schrödinger, E. 1944. What is Life? The Physical Aspects of a Living Cell.- Cambridge
672 University Press.
673 Suurkuusk, J. et al. 2017. The third generation thermal activity monitor (TAM III). - J.
674 Thermal. Anal. Cal. 15: 1-18.

675 Thornton, W. M. 1917. The relation of oxygen to the heat of combustion of organic
676 compounds.- Philos. Mag. 33: 196-203.

677 Villanueva, M. et al. 2011. Energetic characterization of forest biomass by calorimetry and
678 thermal analysis.- J. Thermal. Anal. Cal. 104: 61-67.

679 Voitkevich, O. V. et al. 2012. Thermodynamic properties of plant biomass components.
680 Heat capacity, combustion energy, and gasification equilibria of lignin. – J. Chem. Eng. Data
681 57: 1903-1909.

682 Von Stockar, U. et al. 1993. Calorimetric and energetic efficiencies in aerobic and anaerobic
683 growth.- Pure and Applied Chem. 65: 1889-1892.

684 Von Stockar, U. and Liu, J. S. 1999. Does microbial life always feed on negative entropy?
685 Thermodynamic analysis of microbial growth.- Biochim. Biophys. Acta 1412: 191-211.

686 Von Stockar, U. et al. 2006. Thermodynamics of microbial growth and metabolism: An
687 analysis of the current situation. - J. Biotechnol. 121: 517-533.

688 Wadsö, L. and Hansen, L.D. 2015. Calorespirometry of terrestrial organisms and
689 ecosystems.- Methods 76: 11-19.

690 Walsh, S. 2012. A summary of climate averages for Ireland 1981 – 2010. - Climatological
691 Note No. 14. Met Éireann, Glasnevin Hill, Dublin 9, Ireland.

692

693

694

695

696

697

Samples	DCL/F	GL/F	KL/F	DCH	GH	KH	DCM	GM	KM
OM(%)	95±5	97±5	95±5	82±4	71±3	83±4	7±1	9±1	21±1
T_{50}-DSC (ºC)	370±11	366±11	366±11	391±12	368±11	393±12	340±10	348±10	328±9
T_{50}-TG (ºC)	336±10	335±10	323±9	355±11	327±10	353±11	318±9	322±9	302±9
$-Q_{SOM}$ (kJ/gSOM	15.0±0.5	15.9±0.4	16.4±0.5	16.6±0.5	18.7±0.6	19.3±0.5	26.4±0.7	25.0±0.7	21.3±0.
$-\Delta_C H_{SOM}$ (kJ/Cmol)	422±26	426±24	447±27	452±25	524±27	528±29	639±92	546±62	470±26
$-\Delta_r H_{SOM}$ (kJ/C-CO_2mol)	310±44	327±41	355±51	506±10	462±9	405±13	400±68	485±9	421±17
$\Delta_r H_{SOM}/\Delta_C H_{SOM}$	0.73±0.10	0.77±0.08	0.79±0.10	1.13±0.04	0.88±0.03	0.77±0.03	0.63±0.08	0.89±0.02	0.89±0.
γ_C	3.87	3.91	4.10	4.14	4.81	4.85	5.87	5.00	4.31
γ_r	2.84	3.00	3.26	4.64	4.24	3.72	3.67	4.45	3.86
$-\Delta_C G_{SOM}$ kJ/Cmol	426±26	431±24	452±27	456±25	530±27	535±28	647±92	551±62	475±26
$-\Delta_r G_{SOM}$ (kJ/molC)	356±50	371±46	394±56	525±10	488±9	438±14	433±73	506±9	452±18
$\Delta_c S_{SOM}$ (J/KCmol)	13.4±0.8	16.8±0.9	16.8±1.0	13.4±0.7	20.1±1.0	23.5±1.2	26.9±3.8	16.8±1.9	16.8±0.
$\Delta_r S_{SOM}$ (J/KCmol)	154±21	148±18	131±8	64±1	87±2	111±4	111±19	70±1	104±4
$\delta^{13}C$ ‰	-29.4	-29.4	-29.7	ND	ND	ND	-28.4	-28.7	-28.6
C %	45.45	48.85	46.40	40.50	33.75	40.05	3.70	5.30	12.40
BD (g/cm^3)	ND	ND	ND	0.17±0.02	0.16±0.02	0.15±0.02	1.22±0.05	1.08±0.22	0.66±0.

Table 1: Analytical, thermal and thermodynamic data on the soil samples. DC, G, and K are the samples from Derrycunnihy, Glengarriff and Uragh respectively. L/F corresponds with the aboveground organic litter, H are the humus layer samples, and M the mineral soil samples. Uncertainties are given as the standard deviation of two determinations. The uncertainty in % C is estimated to be ±3% of the value given. $\Delta_C H_{SOM}$ is calculated as (Q_{SOM}+1.839)/[%C/%SOM]*(12 g/mole C). $\Delta_r H_{SOM}$ is calculated as $-R_q/R_{CO2}$. The uncertainty in the degree of reduction for both γ_C and γ_S is estimated to be ±0.3.

Legends for the figures

Figure 1: DSC and DTG curves from all samples. Black lines correspond to L/F samples, red lines to H samples and blue lines to M samples from Derricunnihy (DC plots), Glengarriff (G plots) and Uragh (K plots).

Figure 2: Exo1, Exo2 and char percentages from all samples, representing the labile (Exo1) and recalcitrant (Exo2) fractions of the SOM macromolecule. The percentage of char formed increases following the order L/F < H < M samples in all locations.

Figure 3: Heat rates (R_q) and CO_2 rates (R_{CO2}) of all samples.

Figure 4: Samples distribution based on PCA factor scores in the two-dimensional subspace delimited by the two first components explaining 86 % of the variance.

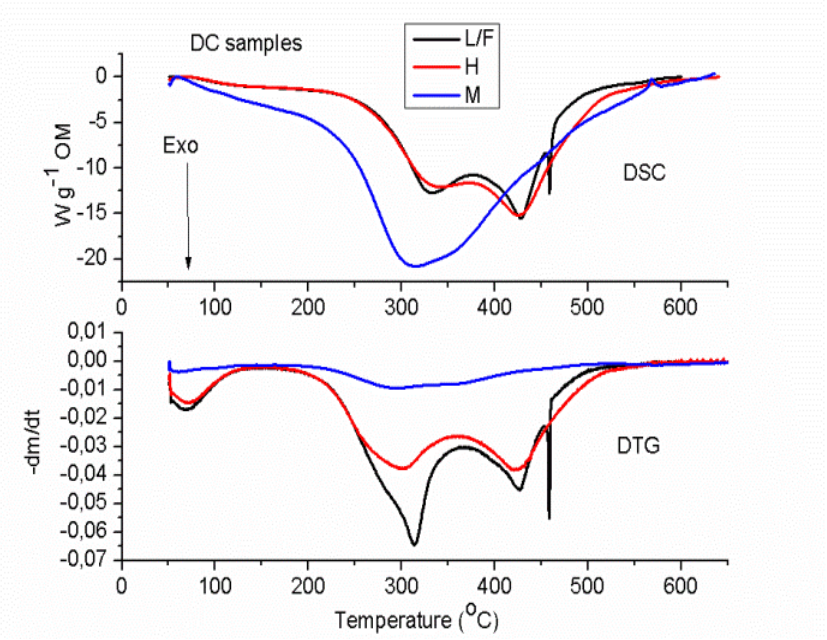
DC samples
L/F
H
M
Exo
DSC
DTG
W g-1 OM
-dm/dt
Temperature (°C)

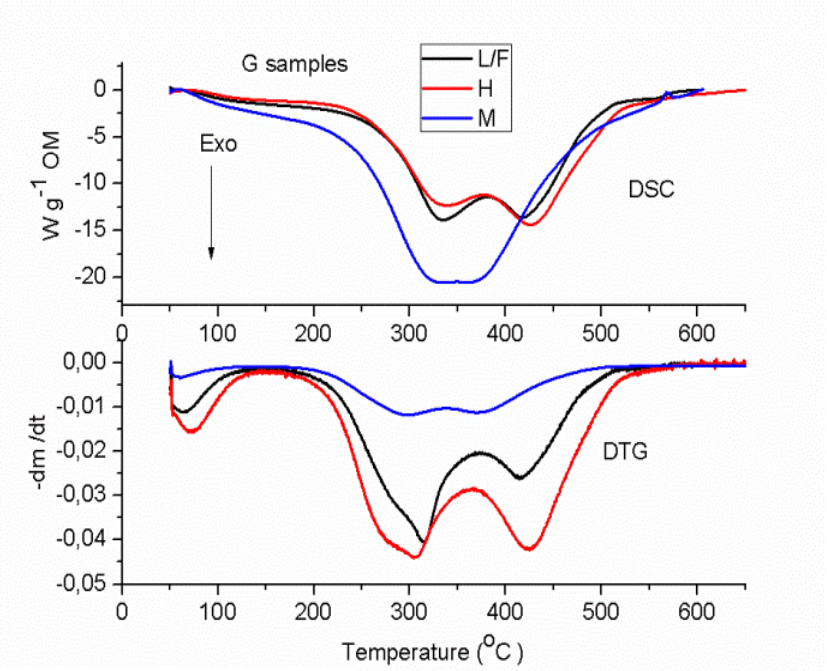
G samples
L/F
H
M
Exo
DSC
DTG
W g-1 OM
-dm /dt
Temperature (°C)

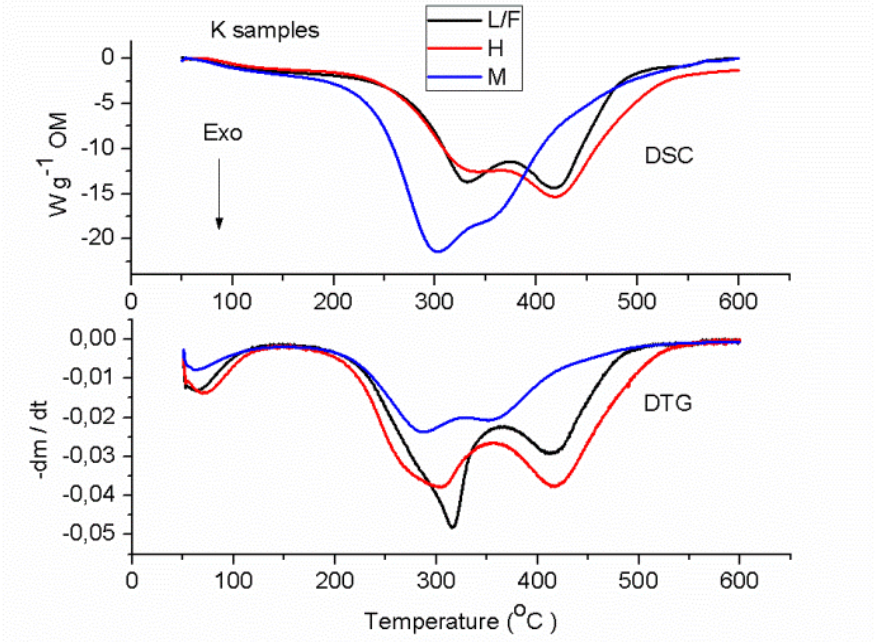
K samples
L/F
H
M
Exo
DSC
DTG
W g-1 OM
-dm / dt
Temperature (°C)

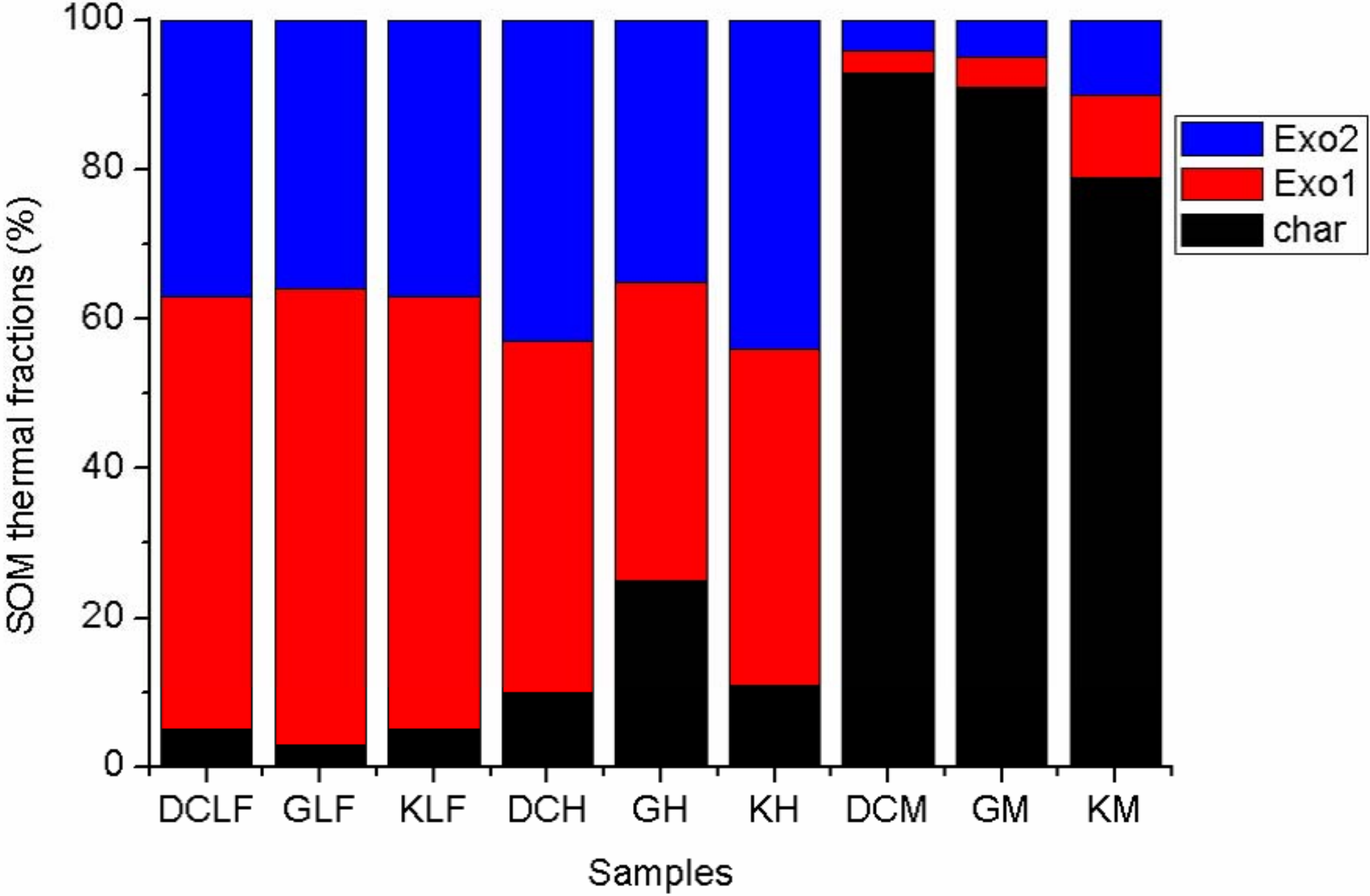
100
80
60
40
20
0
SOM thermal fractions (%)
DCLF
GLF
KLF
DCH
GH
KH
DCM
GM
KM
Samples
Exo2
Exo1
char

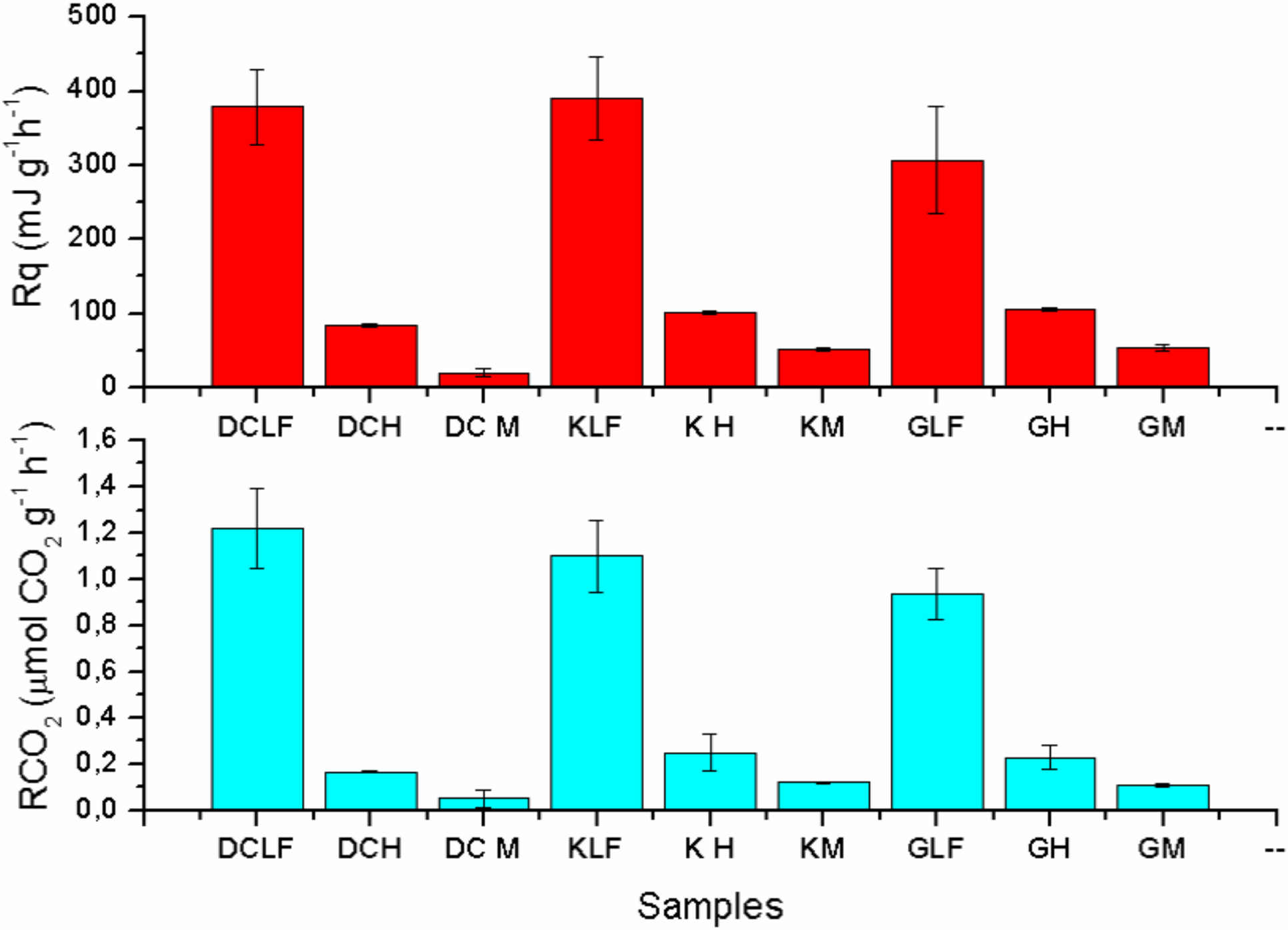
500
400
300
200
100
0
Rq (mJ g-1h-1)
DCLF
DCH
DC M
KLF
K H
KM
GLF
GH
GM
--
1,6
1,4
1,2
1,0
0,8
0,6
0,4
0,2
0,0
RCO2 (µmol CO2 g-1 h-1)
DCLF
DCH
DC M
KLF
K H
KM
GLF
GH
GM
--
Samples

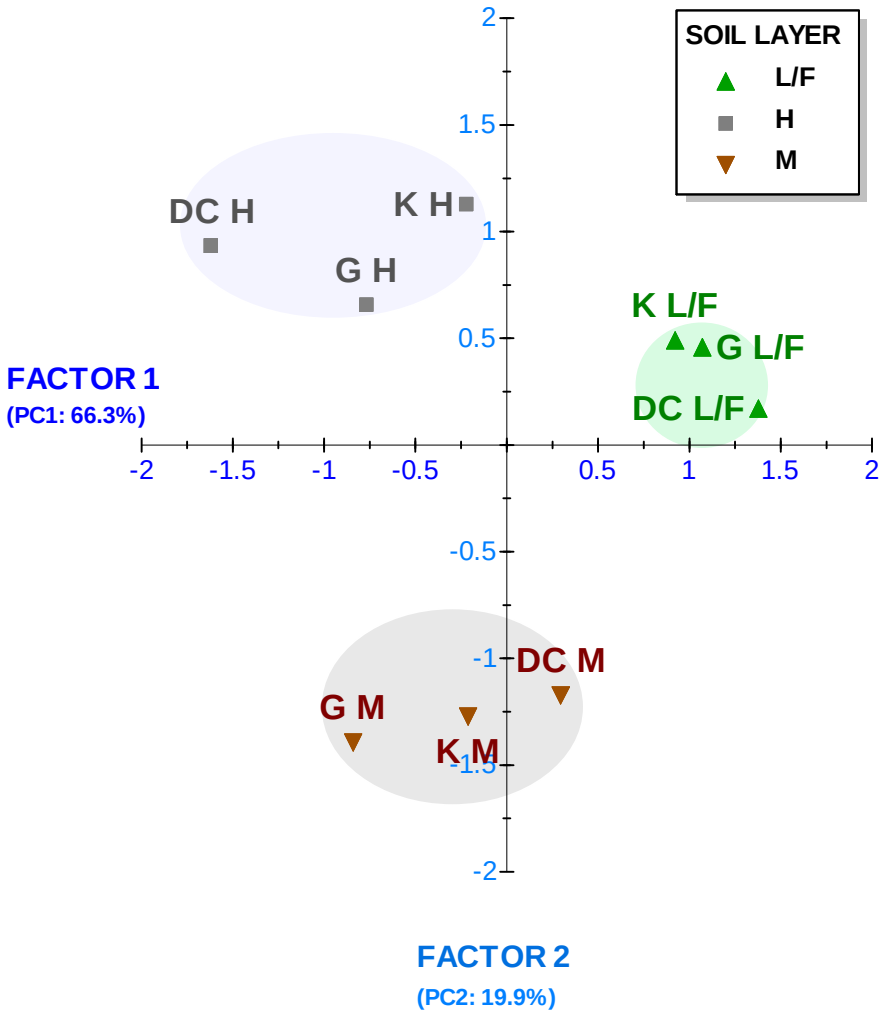

Variable	PC1	PC2
DcHSOM (in the text as: $\Delta_c H_{SOM}$)	-0.307	-0.458
Char	-0.281	-0.926
Exo1	0.403	0.861
Exo2	0.091	0.979
DrHSOM (in the text as: $\Delta_r H_{SOM}$)	-0.984	-0.128
Rq (in the text as: R_q)	0.773	0.417
RCO2 (in the text as: RCO_2)	0.814	0.368
DcSSOM (in the text as: $\Delta_c S_{SOM}$)	-0.006	-0.164
DrSSOM (in the text as: $\Delta_r S_{SOM}$)	0.974	0.159